

# Differential Expression and Cellular Distribution of $\gamma$ -Tubulin and $\beta$ III-Tubulin in Medulloblastomas and Human Medulloblastoma Cell Lines

VALENTINA CARACCILO,<sup>1</sup> LUCA D'AGOSTINO,<sup>1</sup> EDUARDA DRÁBEROVÁ,<sup>2</sup> VLADIMÍRA SLÁDKOVÁ,<sup>2</sup> CATENA CROZIER-FITZGERALD,<sup>1</sup> DIMITRI P. AGAMANOLIS,<sup>3</sup> JEAN-PIERRE DE CHADARÉVIAN,<sup>4,5</sup> AGUSTIN LEGIDO,<sup>4,6</sup> ANTONIO GIORDANO,<sup>1</sup> PAVEL DRÁBER,<sup>2</sup> AND CHRISTOS D. KATSETOS<sup>4,5,6\*</sup>

<sup>1</sup>Sbarro Institute for Cancer Research and Molecular Medicine, Center for Biotechnology, College of Science and Technology, Temple University, Philadelphia, Pennsylvania

<sup>2</sup>Laboratory of the Biology of Cytoskeleton, Institute of Molecular Genetics, Academy of Sciences of the Czech Republic, Prague, Czech Republic

<sup>3</sup>Department of Pathology and Laboratory Medicine, Akron Children's Hospital and Northeastern Ohio Universities College of Medicine, Akron and Rootstown, Ohio

<sup>4</sup>Department of Pediatrics, Drexel University College of Medicine and St. Christopher's Hospital for Children, Philadelphia, Pennsylvania

<sup>5</sup>Department of Pathology and Laboratory Medicine, Drexel University College of Medicine and St. Christopher's Hospital for Children, Philadelphia, Pennsylvania

<sup>6</sup>Department of Neurology, Drexel University College of Medicine, Philadelphia, Pennsylvania

In previous studies, we have shown overexpression and ectopic subcellular distribution of  $\gamma$ -tubulin and  $\beta$ III-tubulin in human glioblastomas and glioblastoma cell lines (Katsetos et al., 2006, *J Neuropathol Exp Neurol* 65:455–467; Katsetos et al., 2007, *Neurochem Res* 32:1387–1398). Here we determined the expression of  $\gamma$ -tubulin in surgically excised medulloblastomas ( $n = 20$ ) and in the human medulloblastoma cell lines D283 Med and DAOY. In clinical tissue samples, the immunohistochemical distribution of  $\gamma$ -tubulin labeling was pervasive and inversely related to neuritogenesis. Overexpression of  $\gamma$ -tubulin was widespread in poorly differentiated, proliferating tumor cells but was significantly diminished in quiescent differentiating tumor cells undergoing neuritogenesis, highlighted by  $\beta$ III-tubulin immunolabeling. By quantitative real-time PCR,  $\gamma$ -tubulin transcripts for TUBG1, TUBG2, and TUBB3 genes were detected in both cell lines but expression was less prominent when compared with the human glioblastoma cell lines. Immunoblotting revealed comparable amounts of  $\gamma$ -tubulin and  $\beta$ III-tubulin in different phases of cell cycle; however, a larger amount of  $\gamma$ -tubulin was detected in D283 Med when compared with DAOY cells. Interphase D283 Med cells exhibited predominantly diffuse cytoplasmic  $\gamma$ -tubulin localization, in addition to the expected centrosome-associated distribution. Robust  $\beta$ III-tubulin immunoreactivity was detected in mitotic spindles of DAOY cells. Our data indicate that overexpression of  $\gamma$ -tubulin may be linked to phenotypic dedifferentiation (anaplasia) and tumor progression in medulloblastomas and may potentially serve as a promising tumor marker.

*J. Cell. Physiol.* 223: 519–529, 2010. © 2010 Wiley-Liss, Inc.

Abbreviations: DAPI, 4',6-diamidino-2-phenylindole; DMEM, Dulbecco's modified Eagle medium; EDTA, ethylene diamine tetraacetic acid; EGTA, ethylene glycol tetraacetic acid; FITC, fluorescein isothiocyanate;  $\gamma$ -TuRC, large  $\gamma$ -tubulin-ring complex;  $\gamma$ -TuSC,  $\gamma$ -tubulin-small complex; LI, labeling index; MTOC, microtubule organizing center; PI, pale islands.

Additional Supporting Information may be found in the online version of this article.

Contract grant sponsor: Sbarro Health Research Organization.  
Contract grant sponsor: Human Health Foundation, Spoleto, Italy.  
Contract grant sponsor: Ministry of Education;  
Contract grant number: IM683780500.  
Contract grant sponsor: Youth and Sports of the Czech Republic.  
Contract grant sponsor: Grant Agency of the Czech Republic;  
Contract grant number: 204/09/1777.

Contract grant sponsor: GA AVCR;  
Contract grant number: KAN200520701.  
Contract grant sponsor: Institutional Research Support;  
Contract grant number: AVOZ 50520514.  
Contract grant sponsor: St. Christopher's Foundation for Children.

\*Correspondence to: Christos D. Katsetos, Professor of Pathology, Drexel University College of Medicine, Section of Neurology, St. Christopher's Hospital for Children, Erie Avenue at Front Street, Philadelphia, PA 19134.  
E-mail: christos.katsetos@drexelmed.edu

Received 20 December 2009; Accepted 22 December 2009

Published online in Wiley InterScience  
(www.interscience.wiley.com.), 16 February 2010.  
DOI: 10.1002/jcp.22077

Medulloblastoma is the archetypal embryonal CNS tumor and the most prevalent malignant brain tumor in children whose origin is traceable to cerebellar neurogenesis (Katsetos and Burger, 1994; Katsetos et al., 1995a, 2003c; Read et al., 2006). Compelling evidence accumulated to date support a fundamentally neuronal/neuroblastic tumor phenotype and a predominantly neuronal differentiation potential (Katsetos and Burger, 1994; Katsetos et al., 2003a; Read et al., 2006). The latter is more pronounced in the nodular/desmoplastic variant of medulloblastoma, which is typified by islands of morphologically differentiating tumor cells undergoing gradations of neuritogenesis (“pale islands”) featuring the co-expression of neuronal marker proteins, including the class III  $\beta$ -tubulin ( $\beta$ III-tubulin), synaptophysin, neurotrophin receptors TrkA and TrkC, low proliferative indices, and apoptosis (Katsetos et al., 1989, 1995b, 2003c; Eberhart et al., 2001).

$\gamma$ -Tubulin is the principal cytoskeletal constituent of the pericentriolar material of centrosomes, the cell’s microtubule-organizing centers (MTOCs) where it plays a central role in microtubule nucleation and also plays a role in the regulation of cell cycle progression (Zhou et al., 2002). Experimental depletion of  $\gamma$ -tubulin leads to a depletion of microtubules and to growth arrest. In mammalian cells, two  $\gamma$ -tubulin genes TUBG1 and TUBG2 exist, encoding two closely related isoforms (Wise et al., 2000). TUBG1 is ubiquitously expressed in all cell types, whereas TUBG2 has been found mainly in the brain (Yuba-Kubo et al., 2005).

Although  $\gamma$ -tubulin is mainly localized on MTOCs, a larger amount of  $\gamma$ -tubulin is in soluble form (Moudjou et al., 1996).  $\gamma$ -Tubulin appears in two main complexes: the large  $\gamma$ -tubulin ring complex ( $\gamma$ TuRC) (Moritz et al., 1995; Zheng et al., 1995) and the  $\gamma$ -tubulin small complex ( $\gamma$ -TuSC) (Moritz et al., 1998). The existence of  $\gamma$ TuRCs correlates with the ability of centrosomes to nucleate microtubules (Schnackenberg and Palazzo, 2001). The  $\gamma$ TuRCs embedded in MTOC matrix nucleate microtubules. In addition to nucleation from MTOC,  $\gamma$ TuRCs are also involved in the regulation of microtubule minus-end dynamics (Wiese and Zheng, 2000).  $\gamma$ -Tubulin has been recognized as a microtubule minus-end binding molecule in non-anchored microtubules (Leguy et al., 2000). In addition,  $\gamma$ -tubulin is associated with cellular membranes (Chabin-Brion et al., 2001; Dryková et al., 2003; Bugnard et al., 2005; Macurek et al., 2008) where it can give rise to non-centrosomal microtubule nucleation (Chabin-Brion et al., 2001; Efimov et al., 2007; Macurek et al., 2008).

$\gamma$ -Tubulin complexes may also be involved in regulating microtubule dynamics and in spindle assembly checkpoint signaling (Prigozhina et al., 2001; Vardy et al., 2002; Müller et al., 2006). Recent findings indicate that the dynamics of microtubule plus-ends are altered, depending on the expression of  $\gamma$ -tubulin complex proteins (reviewed in Raynaud-Messina and Merdes, 2007; Bouissou et al., 2009). Overlapping role of  $\gamma$ -tubulin with C-terminal kinesin-like protein Pkl1 in bipolar spindle formation has been reported (Paluh et al., 2000; Rodriguez et al., 2008). Cell cycle-dependent accumulation of  $\gamma$ -tubulin has been described previously (Binarová et al., 2000; Schröder et al., 2002).

The role of  $\gamma$ -tubulin in microtubule nucleation and microtubule nucleation-independent function in non-transformed cells as well as the altered expression, distribution, and subcellular sorting of this protein in cancer cells have been reviewed recently (Katsetos et al., 2009a). In previous studies, we have shown overexpression and ectopic compartmentalization of  $\gamma$ -tubulin in astrocytic gliomas, especially in glioblastoma multiforme, and have suggested that this can be a putative mechanism of malignancy and tumor progression (Katsetos et al., 2006, 2007, 2009a). Moreover, we have previously shown that  $\gamma$ -tubulin is co-distributed with

class III  $\beta$ -tubulin ( $\beta$ III-tubulin) in high-grade gliomas (anaplastic astrocytomas and glioblastomas multiforme) and have suggested that aberrant expression and interaction of these two cytoskeletal proteins may be linked to malignant changes in glial cells (Katsetos et al., 2007).

To get a broader insight into the expression of this protein in brain tumors, we have analyzed the expression and cellular distribution of  $\gamma$ -tubulin and its relation to  $\beta$ III-tubulin in surgically excised medulloblastomas and the human medulloblastoma cell lines D283 Med and DAOY.

## Materials and Methods

### Cell lines

Medulloblastoma cell lines, DAOY and D283 Med, were purchased from the American Type Culture Collection (ATCC; Manassas, VA). DAOY (No. HTB-186) was isolated from a posterior fossa tumor of a 4-year-old boy; D283 Med (No. HTB-185) originated from peritoneal metastases from a boy with medulloblastoma (Katsetos et al., 1995a). The cells were grown in Dulbecco’s modified Eagle’s medium (DMEM; CellGro; Mediatech, Inc., Herndon, VA) containing 10% (v/v) fetal bovine serum (FBS; Atlanta Biological; Norcross, GA) at 37°C and 5% CO<sub>2</sub> atmosphere and passaged every 2–3 days using 0.25% trypsin–EDTA solution (Sigma, St. Louis, MO).

Proliferating non-immortalized, non-transformed human fetal astrocytes (NHA; Clonetics<sup>®</sup> Astrocyte Cell Systems) commercially obtained from Lonza (Walkersville, MD) and cells from the human glioblastoma cell line U138MG and human osteogenic sarcoma cell line U-2OS obtained from ATCC, were used as controls for the quantitative real-time PCR (qRT-PCR) experiments (see below).

NHA cells were maintained as monolayer cultures in tissue culture flasks for 8–10 days in an astrocyte growth medium (CC-3186; Clonetics<sup>®</sup> AGM<sup>™</sup> Bullet Kit), containing astrocyte basal medium<sup>™</sup> (CCMD 190, Clonetics<sup>®</sup>) and the following growth supplements: human recombinant growth factor (rhEGF), insulin, ascorbic acid, gentamycin–amphotericin B (GA-1000), L-glutamine, and 5% FBS, according to manufacturer’s instructions.

Human glioblastoma cell line U138MG (ATCC), human osteogenic sarcoma cells U-2OS (ATCC), human neuroblastoma SH-SY5Y (ATCC), and human kidney embryonal cells HEK293-FT (Promega, Madison, WI) were cultured in DMEM containing 10% (v/v) FBS, penicillin (100 units/ml), and streptomycin (0.1 mg/ml). Cells were grown at 37°C in 5% CO<sub>2</sub> in air and passaged every 3 days using 0.25% (w/v) trypsin/0.01% (w/v) EDTA in phosphate-buffered solution (PBS), pH 7.5.

### Clinical tissue samples

Formaldehyde (formalin)-fixed, paraffin-embedded biopsy/resection samples of medulloblastoma (n = 20) were collected retrospectively from St. Christopher’s Hospital for Children (Philadelphia, PA) and Akron Children’s Hospital (Akron, OH) between 1990 and 2000 under the approval of the Drexel University College of Medicine Institutional Review Board. Thirteen patients were male and seven female. At resection, the median age of the patients was 5.4 years (range 18 months to 12 years). Histological classification was according to the recommendations of the Pediatric Oncology Group study on histopathologic grading of medulloblastomas (Eberhart et al., 2002) and of the 2007 World Health Organization (WHO) classification of tumors of the central nervous system (Louis et al., 2007). Twelve tumors were classified as classic, two as large cell/anaplastic, and six as nodular/desmoplastic medulloblastomas. The latter were typified by a biphasic nodular architecture comprised of loosely textured, finely fibrillated/reticulin-free islands of neuronal differentiation (“pale islands”) surrounded by reticulin-impregnated, densely populated solid sheets of poorly

differentiated tumor cells (Katsetos and Burger, 1994; Katsetos et al., 2003c).

Non-neoplastic cerebellar autopsy tissue samples ( $n = 10$ ) were examined from five fetuses (24-, 28-, 32-, 36-, and 38-weeks of gestation), three infants (2-, 4-, and 8-months of age), and two children (6 and 7 years old) who had died of non-neurological conditions. The utility of autopsy tissues met the approval of the Drexel University College of Medicine Institutional Review Board.

Histologic preparations were evaluated independently by two neuropathologists (DPA and CDK) and a pediatric pathologist (JPD) who were blinded as to the pathological diagnosis originally rendered for each specimen.

### Antibodies

For the detection of  $\gamma$ -tubulin, polyclonal and monoclonal anti-peptide antibodies recognizing distinct epitopes in the C-terminus of the  $\gamma$ -tubulin molecule were used. These included a rabbit polyclonal antibody DQ-19 to amino acid sequence 433-451 (Sigma, T3195) and three monoclonal antibodies TU-30 (IgG2b), TU-31 (IgG2b), and TU-32 (IgG1) recognizing different epitopes in the amino acid sequence 434-449 (Nováková et al., 1996). The specificity of these anti- $\gamma$ -tubulin antibodies has been extensively characterized and verified in various cell types (Sulimenko et al., 2002; Libusová et al., 2004). The monoclonal antibody supernatants were stored in freeze-dried state in the presence of trehalose (Dráber et al., 1995).

For the detection of class III  $\beta$ -tubulin ( $\beta$ III-tubulin), two antibodies were used. Mouse monoclonal antibody TuJ1 (IgG2a) is directed against an epitope on the C-terminus of the neuron-specific  $\beta$ III-tubulin. The characterization, purification, and production of TuJ1 has been described elsewhere (Lee et al., 1990a,b; Alexander et al., 1991). The predominantly neuronal cell type distribution of monoclonal antibody TuJ1 in developing and mature, non-neoplastic human tissues has been elucidated in previous studies (Katsetos et al., 1993, 1998, 2003a,b). In addition, an affinity purified rabbit antibody against the CMYEDDDDESEAQGPK peptide identical to the  $\beta$ III carboxyl terminal, isotype-defining domain detected by monoclonal antibody TuJ1, was used (Katsetos et al., 2000).

Monoclonal antibody PC10 to proliferating cell nuclear antigen (PCNA)/cyclin (PC-10 sc-56) (Santa Cruz Biotechnologies, Inc., Santa Cruz, CA; Katsetos et al., 1995b) was used as a marker of cell proliferation. Goat polyclonal anti-actin (I-19, sc-16116; Santa Cruz Biotechnologies, Inc.) or mouse monoclonal anti-Grb2 (BD 610112; BD Biosciences, San Jose, CA) were used in immunoblots as internal controls for total protein extracts.

Secondary fluorochrome-conjugated goat-anti-rabbit AlexaFluor 594 (red) and goat-anti-mouse AlexaFluor 488 (green) were purchased from Invitrogen (Carlsbad, CA). FITC-conjugated anti-rabbit and Cy3-conjugated anti-mouse antibodies were from Jackson ImmunoResearch Laboratories (West Grove, PA). Secondary anti-mouse and anti-rabbit antibodies conjugated with horseradish peroxidase were purchased from Pierce (ThermoFisher Scientific, Rockford, IL).

### Immunohistochemistry on clinical tumor samples

Immunohistochemistry was performed according to the avidin biotin complex (ABC) peroxidase method using Rabbit and Mouse IgG ABC Elite<sup>®</sup> detection kits (Vector Laboratories, Burlingame, CA) as previously described (Katsetos et al., 2006, 2007). Prior to the performance of the immunohistochemical procedure, 5- $\mu$ m thick histological sections from paraffin-embedded tissue blocks were subjected to non-enzymatic antigen unmasking in 0.01 M sodium citrate buffer (pH 6.0) for 10 min in a microwave at medium power. The rabbit polyclonal antibody to  $\gamma$ -tubulin (DQ-19) was used at a 1:500 dilution whereas anti- $\gamma$ -tubulin monoclonal antibodies TU-30, TU-31, and TU-32 were used as undiluted supernatants. Both monoclonal antibody TuJ1 and rabbit polyclonal

antibody to  $\beta$ III-tubulin were used at a working dilution of 1:500. Monoclonal antibody PC10 to PCNA was used at a dilution of 1:100. Negative controls included the omission of primary antibody and substitution with non-specific mouse IgG1 and IgG2a and IgG2b, which were used as immunoglobulin class-specific controls (corresponding to the immunoglobulin subclasses of the primary antibodies employed in this study) (Becton Dickinson, Franklin Lakes, NJ). Experiments using non-conjugated isotype-matched control monoclonal antibodies did not show any non-specific binding of the secondary rabbit anti-mouse IgG1, IgG2a, or IgG2b antibodies.

Manual cell counting of labeled tumor cells was performed by three observers independently (VC, LD, CDK). Cell counting and statistical analysis were carried out in all medulloblastoma specimens ( $n = 20$ ) with all antibodies employed in this study. Between 650 and 1,115 tumor cells were evaluated per case, in 20 non-overlapping high-power ( $40\times$ ) fields and labeling indices (LIs) were generated per each specimen. LI was expressed as the percentage (%) of either  $\beta$ III-tubulin or  $\gamma$ -tubulin labeled cells out of the total number of tumor cells counted in each case and for each antibody. The minimal criterion for the identification of a  $\gamma$ -tubulin-positive cell in the context of an abnormal staining pattern associated with putative centrosome dysfunction was the detection of three or more punctate, dot-like immunoreactive signals, and/or robust diffuse staining, in the cytoplasm of individual tumor cells as previously described (Katsetos et al., 2006).

A semi-quantitative analysis of the immunohistochemical findings was made by evaluating the LIs according to a simplified and readily reproducible three tier-scoring system as follows:  $-$ , no staining;  $+$ , labeling of a small number of tumor cells (LI  $<20\%$ );  $++$ , labeling of an intermediate number of tumor cells (LI: 20–60%);  $+++$ , labeling of a large number of tumor cells (LI  $\geq 60\%$ ). Interobserver agreement for the evaluation of immunohistochemical staining was within 10% ( $k = 0.82$ ).

### Immunofluorescence on clinical tumor samples

Sections from formaldehyde-fixed, paraffin-embedded tumor tissues obtained after surgical resection were utilized for immunofluorescence microscopy as described previously (Katsetos et al., 2006). Deparaffinized sections were incubated for 50 min in a freshly made PBS solution containing 1 mg/ml of sodium borohydride (Sigma) to decrease the autofluorescence, and subsequently they were rinsed extensively with PBS. For double-labeling immunofluorescence studies on histological sections, rabbit polyclonal anti- $\gamma$ -tubulin antibody and mouse monoclonal anti- $\beta$ III-tubulin antibody (TuJ1) were diluted 1:500. Secondary fluorochrome conjugated antibodies included anti-rabbit AlexaFluor 594 and anti-mouse AlexaFluor 488, respectively, and were diluted 1:600 with PBS. Double staining was performed in two sequential sessions of immunofluorescence staining. 4',6-diamidino-2-phenylindole (DAPI) was used to label cell nuclei. Slides were cover-slipped using an aqueous-based mounting medium (Vector Laboratories).

### Immunofluorescence staining on cell lines

Cells grown on coverslips were rinsed in PBS and fixed with 4% paraformaldehyde at room temperature for 20 min. After rinsing with PBS, they were incubated with 0.1% Triton X-100 at room temperature for 10 min to permeabilize the cell membrane and rinsed again with PBS. Cells were incubated in blocking solution (6% BSA in PBS) for 1 h at room temperature and then with primary antibody overnight at 4°C. The primary antibodies were rabbit polyclonal anti- $\gamma$ -tubulin and mouse monoclonal anti- $\beta$ III-tubulin as for immunohistochemistry. The slides were rinsed three times with PBS and incubated for 1 h at room temperature with secondary fluorochrome-conjugated antibodies anti-rabbit AlexaFluor 594 and anti-mouse AlexaFluor 488, respectively. DAPI was used to label cell nuclei. The preparations were mounted with

Vectashield mounting medium (Vector Laboratories) and examined with an Olympus IX81 deconvolution fluorescence microscope (Olympus Microscopes, Center Valley, PA). No staining was detected when conjugates alone were used as negative controls.

Alternatively, cells grown on coverlips were fixed in cold methanol and double-label stained (Dráber et al., 1989) with monoclonal anti- $\gamma$ -tubulin antibody TU-30 (undiluted supernatant) and polyclonal anti- $\beta$ III-tubulin antibody (1:500). A secondary anti-mouse antibody, conjugated with Cy3, and an anti-rabbit antibody, conjugated with FITC, were diluted, respectively, 1:500 and 1:200.

#### Cell synchronization

In order to obtain a synchronous population of cells, confluent plates of DAOY cells were incubated with DMEM containing only 0.1% FBS for 72 h. The medium was then changed with DMEM containing 10% FBS and 2 mM of hydroxyurea (Sigma). The treatment with hydroxyurea lasted for 21 h. The cells were then replated in new plates and samples of cells were collected each hour for FACS analysis, to identify the best time point for G0/G1, S, and G2/M phases of the cell cycle, and the corresponding pellets were used for Western blot (immunoblot) analysis.

#### Immunoblot analysis

Protein samples (50  $\mu$ g/lane) from asynchronously growing cells, or samples from synchronized cells were run on polyacrylamide gels according to Laemmli procedure (Laemmli, 1970). Protein bands were transferred on nitrocellulose membranes (Schleicher & Schuell, Dassel, Germany) by wet electrophoretic transfer according to Towbin (Towbin et al., 1979). Non-specific binding sites were blocked for 1 h at room temperature with 5% no fat dry milk in TBS containing 0.05% Tween-20 (TBS-T). The blots were probed with the following primary antibodies at appropriate dilutions: rabbit polyclonal anti- $\gamma$ -tubulin 1:1,000, mouse monoclonal  $\beta$ III-tubulin (TuJ1) 1:2,000, goat polyclonal anti- $\beta$ -actin 1:200, and mouse monoclonal anti-GRB-2 1:4,000. All primary antibodies were diluted in 5% no fat dry milk in TBS-T and incubated overnight at 4°C. After extensive washings, the blots were incubated with secondary anti-mouse or anti-rabbit or anti-goat peroxidase-conjugated antibodies (Amersham; Buckinghamshire, UK) diluted 1:10,000 in TBS-T containing 5% no fat dry milk, for 1 h at room temperature. After rinsing, immune reactive bands were visualized by ECL (Amersham, Buckinghamshire, UK).

#### Quantitative RT-PCR analysis

Total RNA from cell lines and NHA were isolated by the RNeasy Mini kit (QIAGEN, Valencia, CA). Aliquots of 1  $\mu$ g of total RNA in 20  $\mu$ l reaction mixture were converted to cDNA using the ImProm-II RT kit (Promega) with random hexamers. Twenty microliters of the cDNA reaction mixture was diluted five times in DEPC-treated water to prevent the inhibition of Taq polymerase in subsequent PCR reaction. One microliter of diluted cDNA product was used in each PCR reaction. Amplifications were performed in 10  $\mu$ l PCR reaction mixtures containing QuantiTect SYBR Green PCR Master Mix (QIAGEN) and 0.5  $\mu$ M of each human gene-specific primers for  $\gamma$ -tubulin 1 (TUBG1, Refseq ID: NM\_001070),  $\gamma$ -tubulin 2 (TUBG2, Refseq ID: NM\_016437),  $\beta$ III-tubulin (TUBB3, Refseq ID: NM\_006086), or GAPDH (GAPDH, Refseq ID: NM\_002046). Primer sequences are summarized in Table 1. Oligonucleotides were from East Port (Czech Republic). qRT-PCRs were carried out on Master-cycler realplex (Eppendorf) as described (Dráberová et al., 2008). Experiments were performed twice with triplicate samples (cDNA isolated from three separate cultures of tested cells). The expression of analyzed genes was normalized to the expression of GAPDH. Levels of GAPDH did not differ significantly between cell lines and NHA.

TABLE 1. Sequence of Oligonucleotides Used for RT-qPCR

Name	Sequence
$\gamma$ -Tubulin 1, forward	5'-CCCTCATCTGCCTTACTGGTTG-3'
$\gamma$ -Tubulin 1, reverse	5'-AGGTCCCTGATCTGTGCTCTGA-3'
$\gamma$ -Tubulin 2, forward	5'-GGAGCTCATTGATGAGTACCATG-3'
$\gamma$ -Tubulin 2, reverse	5'-AGGAGAAGGAGTAGTGGGGAG-3'
$\beta$ III-Tubulin, forward	5'-GCGAGATGTACGAAGACGAC-3'
$\beta$ III-Tubulin, reverse	5'-TTTAGACACTGCTGGCTTCG-3'
GAPDH, forward	5'-ATGGGGAAGGTGAAGGTCGG-3'
GAPDH, reverse	5'-GACGGTGCCATGGAATTTGC-3'

Identity of  $\gamma$ -tubulin 1 and  $\gamma$ -tubulin 2 PCR products was verified by sequencing. Statistical analysis was performed with the Student's unpaired t-test.

## Results

### Distribution of $\gamma$ -tubulin and $\beta$ III-tubulin in clinical tumor specimens

Immunohistochemical and immunofluorescence analysis of surgically excised clinical tissue samples of medulloblastoma showed pervasive and robust  $\gamma$ -tubulin expression with distinct patterns of cellular localization among differentiating tumor phenotypes. Accordingly, widespread and markedly intense  $\gamma$ -tubulin immunoreactivity with mean LI of  $82 \pm 8\%$  (+++) was identified in solid sheets of poorly differentiated tumor cells exhibiting high tumor cell density (Fig. 1A,B). These sheets comprised actively proliferating tumor cells exhibiting widespread PCNA nuclear staining with a mean LI of  $77 \pm 9\%$  (+++) (Fig. 1C,F) similar to that previously reported (Katsetos et al., 1995b). Identical patterns of immunoreactivity were obtained with different polyclonal and monoclonal anti- $\gamma$ -tubulin antibodies employed in this study.

Varying degrees of overlap were observed between  $\gamma$ -tubulin and  $\beta$ III-tubulin immunoreactivity profiles both in populations of small apolar tumor cells and in slightly polar cells with incipient growth cone-like processes (Fig. 1D,E). However, divergent  $\gamma$ -tubulin and  $\beta$ III-tubulin localizations were observed in Homer Wright (neuroblastic) rosettes. These centripetal neoplastic structures with fibrillary cores, comprised tangles of fasciculating neurites, were consistently and strongly  $\beta$ III-tubulin-positive (Fig. 2A) but were either  $\gamma$ -tubulin-negative or exhibited weak and inconsistent  $\gamma$ -tubulin fibrillary immunostaining (Fig. 2B). Tumor cells forming Homer Wright rosettes displayed variously prominent nuclear PCNA labeling (Fig. 2C).

Differential patterns of cellular localization of  $\gamma$ -tubulin and  $\beta$ III-tubulin were observed within geographic areas typifying the nodular/desmoplastic medulloblastomas. In nodular/desmoplastic medulloblastomas, the cellular distribution of  $\gamma$ -tubulin was prominent in tightly packed sheets of poorly differentiated and cycling PCNA-positive tumor cells (identical to classic medulloblastomas), when compared with foci of tumor neurogenesis ("pale islands") that were strongly immunoreactive for  $\beta$ III-tubulin (Fig. 3C,D) and for the most part,  $\gamma$ -tubulin-negative (Figs. 3A,B and 4B). PCNA labeling was also significantly diminished or was essentially negative in the "pale islands" (Fig. 4A). The inverse pattern of localization of  $\gamma$ -tubulin and  $\beta$ III-tubulin was further confirmed by double-label immunofluorescence microscopy (Fig. 4C). Perikaryal  $\gamma$ -tubulin staining was detected in a small population of randomly scattered tumor cells within the "pale islands" featuring small hyperchromatic nuclei (Fig. 3B). These isolated cells were integrally comingled with differentiating cells with larger vesicular nuclei and elongated axon-like processes exhibiting robust  $\beta$ III-tubulin immunoreactivity (Fig. 3D). A statistically significant difference in  $\gamma$ -tubulin,  $\beta$ III-tubulin, and PCNA LIs was detected between solid tumor areas and "pale islands"



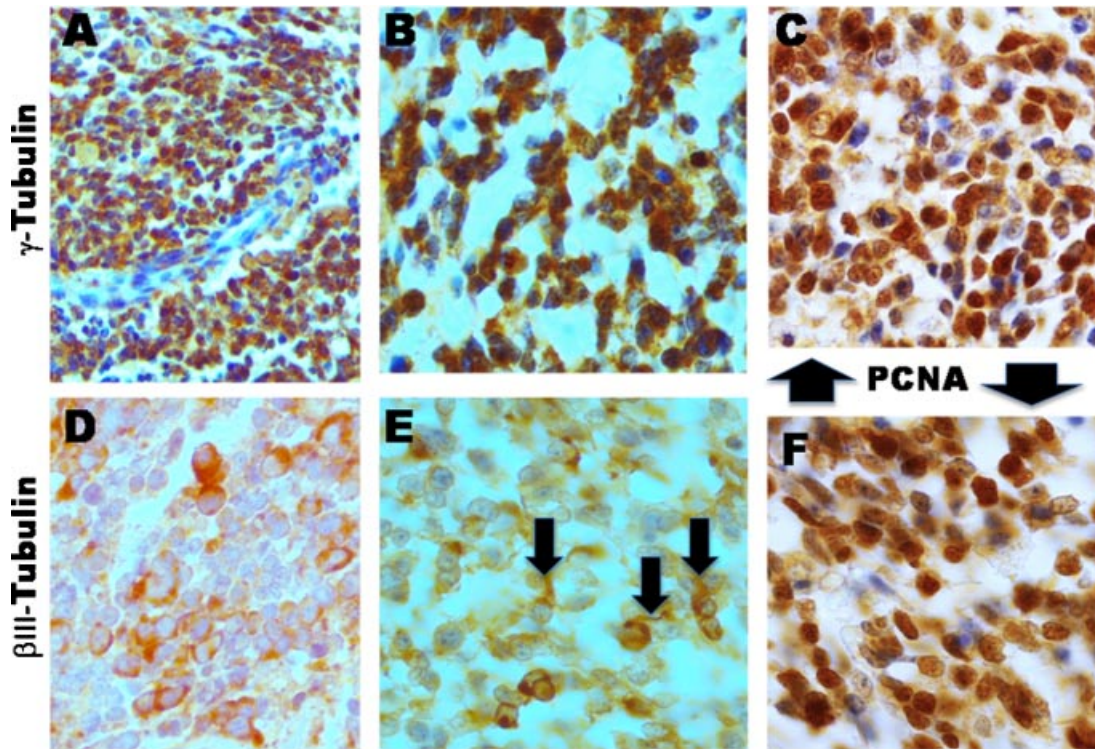


**Fig. 1.** Patterns of  $\gamma$ -tubulin and  $\beta$ III-tubulin distribution in classic medulloblastomas. Parts A and B show widespread cytoplasmic  $\gamma$ -tubulin immunoreactivity in sheets of poorly differentiated tumor cells. Parts D and E depict  $\beta$ III-tubulin labeling in populations of small apolar tumor cells and slightly polar cells with incipient growth cone-like processes (arrows). Actively proliferating tumor cells are shown in C and F. Avidin biotin complex (ABC) peroxidase with hematoxylin counterstain. Original magnifications: A, 400 $\times$ ; B–F, 1,000 $\times$ .

( $P < 0.001$  vs.  $\beta$ III-tubulin,  $P < 0.005$  vs. PCNA). However, when compared group-for-group with combined LIs obtained from both tumor components of nodular/desmoplastic medulloblastomas, no statistically significant differences with regard to  $\gamma$ -tubulin LIs were found between the two major medulloblastoma subtypes. This is attributed to the fact that, in the nodular/desmoplastic variant, differentiating foci are

overgrown by solid areas comprised of poorly differentiated and actively cycling tumor cells. The differential distribution of  $\gamma$ -tubulin,  $\beta$ III-tubulin, and PCNA in the different histological components of nodular/desmoplastic medulloblastomas is summarized in Figure 4D.

Diffuse  $\gamma$ -tubulin immunoreactivity was detected in the mitotically active neuronal precursor cells (neuroblasts) of the

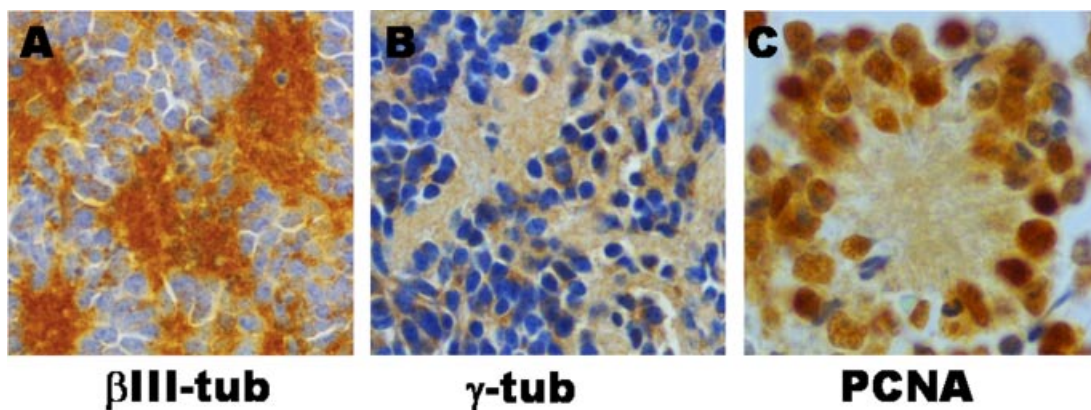


**Fig. 2.** Homer Wright (neuroblastic) rosettes exhibiting strong  $\beta$ III-tubulin labeling (A) and lack of  $\gamma$ -tubulin immunoreactivity (B) in fibrillary cores. Note variously prominent PCNA labeling in the nuclei of tumor cells forming Homer Wright rosettes (C). ABC peroxidase with hematoxylin counterstain. Original magnifications: A–C, 1,000 $\times$ .

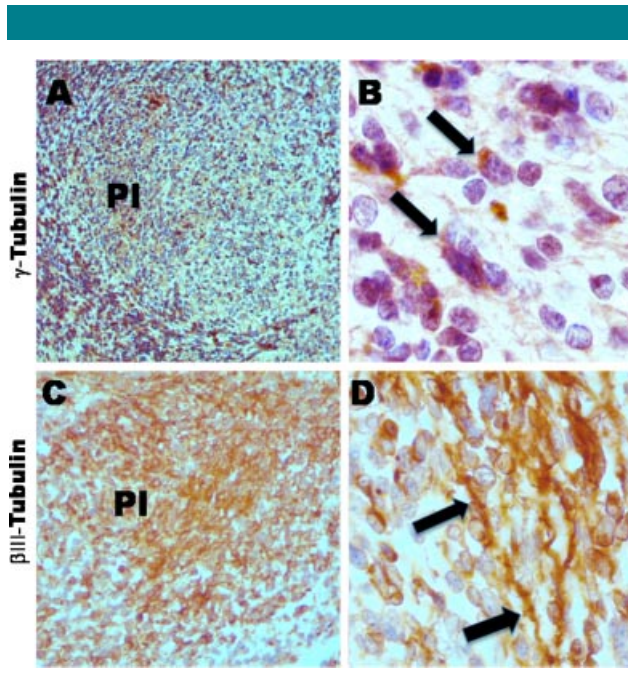


**Fig. 3. Divergent patterns of immunolocalization of  $\gamma$ -tubulin and  $\beta$ III-tubulin in nodular/desmoplastic medulloblastomas. Distribution of  $\gamma$ -tubulin is prominent in poorly differentiated tumor cells surrounding foci of tumor neurogenesis (“pale islands”) (PI) (A). Pale islands are strongly immunoreactive for  $\beta$ III-tubulin (C,D). Within the pale islands,  $\gamma$ -tubulin staining is detected in the perinuclear cytoplasm (protoperikaryon) of scattered tumor cells with hyperchromatic nuclei (B), which are admixed with neurite-bearing tumor cells with larger vesicular nuclei with robust fibrillary  $\beta$ III-tubulin immunoreactivity (D). ABC peroxidase with hematoxylin counterstain. Original magnifications: A, 200 $\times$ ; B,D, 1,000 $\times$ ; C, 400 $\times$ .**

external granule layer, coupled with weak perikaryal staining of Purkinje cells and single dot-like staining in Golgi II neurons and in basket, stellate, and granule cells in the non-neoplastic cerebellar cortex (not shown).

#### Differential localization of $\gamma$ -tubulin and $\beta$ III-tubulin in medulloblastoma cell lines

The expression and distribution of  $\gamma$ -tubulin was evaluated in two well-established medulloblastoma cell lines, DAOY and D283 Med, widely used as representative cell lines in studies related to medulloblastoma during the past two decades. The former shows neuronal and glial differentiation whereas the latter exhibits solely neuronal differentiation potential (He et al., 1989; Peyrl et al., 2003). Typical immunocytochemical localizations of  $\gamma$ -tubulin in interphase medulloblastoma cell lines DAOY and D283 Med are shown in Figure 5. Although, in DAOY cells,  $\gamma$ -tubulin was mainly concentrated in MTOC (Fig. 5A), D283 Med cells exhibited predominantly diffuse cytoplasmic  $\gamma$ -tubulin localization, in addition to the MTOC distribution (Fig. 5D). Similar staining patterns were observed both with polyclonal and monoclonal anti- $\gamma$ -tubulin antibodies. In DAOY cells, grown on coverslips as monolayers,  $\beta$ III-tubulin labeling was detected both in microtubules and in the cytoplasmic pool (Fig. 5B). In D283 Med cells, grown as suspensions,  $\beta$ III-tubulin had solely a diffuse cytoplasmic localization and was not associated with interphase microtubules (Fig. 5E). Although more intensive  $\beta$ III-tubulin staining was detected in majority of DAOY cells when compared with D283 Med cells (Fig. 5B,E), a population of mostly unipolar D283 cells with incipient growth cone-like

processes that could easily adhere onto coverslips was strongly stained for  $\beta$ III-tubulin (see supporting information Fig. S1).

Immunofluorescent double staining revealed that although both  $\gamma$ -tubulin and  $\beta$ III-tubulin were expressed in both cell lines, no obvious co-localization of these proteins was detected (Fig. 5C,F). In mitotic DAOY cells, robust  $\beta$ III-tubulin immunoreactivity was detected in spindle microtubules of cells in metaphase (Fig. 6A,B) and anaphase where it was flanked by two  $\gamma$ -tubulin immunoreactive centrosomes (Fig. 6B,C), as well as in cells in telophase and midbody of cytokinesis (Fig. 6D). Morphologically, DAOY and D283 Med cells in mitosis also exhibited diffusely abundant cytoplasmic  $\gamma$ -tubulin staining (Fig. 6C,D).

By immunoblotting, in asynchronously growing medulloblastoma cell lines, the  $\gamma$ -tubulin expression was more prominent in D283 Med cells when compared with DAOY cells. On the other hand, more  $\beta$ III-tubulin was found in DAOY cells (Fig. 7). In order to follow the distribution of  $\gamma$ -tubulin and  $\beta$ III-tubulin throughout the different phases of the cell cycle, synchronization experiments were performed in DAOY cells. The cell cycle profiles of DAOY cells in asynchronous growth (AG), after 72 h serum deprivation and hydroxyurea treatment (72 h SD + HU), after 10 h (10 h rel) and after 29 h release (29 h rel) from the G0/G1 are shown in Figure 8 (part I). The distribution of the percentage of cells in the different phases of the cell cycle for each condition is shown in part II of Figure 8. Immunoblot analysis of synchronized DAOY cells revealed no substantial changes in the amount of  $\gamma$ -tubulin and  $\beta$ III-tubulin in G0/G1, S, and G2/M phases of the cell cycle (Fig. 9). Putative proteolytic fragments of  $\beta$ III-tubulin were also detected (Fig. 9).

By RT-qPCR,  $\gamma$ -tubulin transcripts for TUBG1 and TUBG2 genes were detected in both D283 Med and DAOY cells. Transcripts for both  $\gamma$ -tubulin genes were slightly more abundant in D283 Med cells. However, expression in medulloblastoma cell lines was less prominent when compared with human glioblastoma cell line U138MG (Fig. 10). Similarly, the expression level of mRNA for  $\beta$ III-tubulin in medulloblastoma cell lines was less prominent when compared with U138MG cells or neuroblastoma cells SH-SY5Y, used as positive control. Slightly higher expression of  $\beta$ III-tubulin was present in DAOY cells when compared with D283 Med cells (see supporting information Fig. S2).

#### Discussion

In previous studies, we have shown aberrant expression and cytoplasmic accumulation of  $\gamma$ -tubulin and  $\beta$ III-tubulin in astrocytic gliomas according to an ascending scale of histological malignancy (Katselos et al., 2006, 2007, 2009a). Moreover, overexpression and perturbations in the subcellular distribution of  $\gamma$ -tubulin in glioblastoma multiforme, the most common malignant brain tumor in adults, suggest that  $\gamma$ -tubulin amplification may be a pivotal mechanism underlying tumorigenesis and tumor progression in gliomas (Katselos et al., 2006, 2007, 2009a). The present study is, to our knowledge, the first to demonstrate overexpression of  $\gamma$ -tubulin also in medulloblastomas and medulloblastoma cell lines.

Unlike gliomas/glioblastomas, which are phenotypically glial neoplasms, medulloblastomas exhibit predominantly neuronal/neuroblastic phenotypes and neuronal differentiation potential, which recapitulates cerebellar neurogenesis (Katselos et al., 2003c; Read et al., 2006). Morphologically, medulloblastomas display varying degrees of neuritic development typified by Homer Wright (neuroblastic) rosettes and areas of neoplastic neurogenesis referred to as “pale islands.” The latter are highlighted by robust immunostaining for  $\beta$ III-tubulin, a marker of neuronal phenotypes in the context of growth and differentiation of medulloblastomas, as well as other



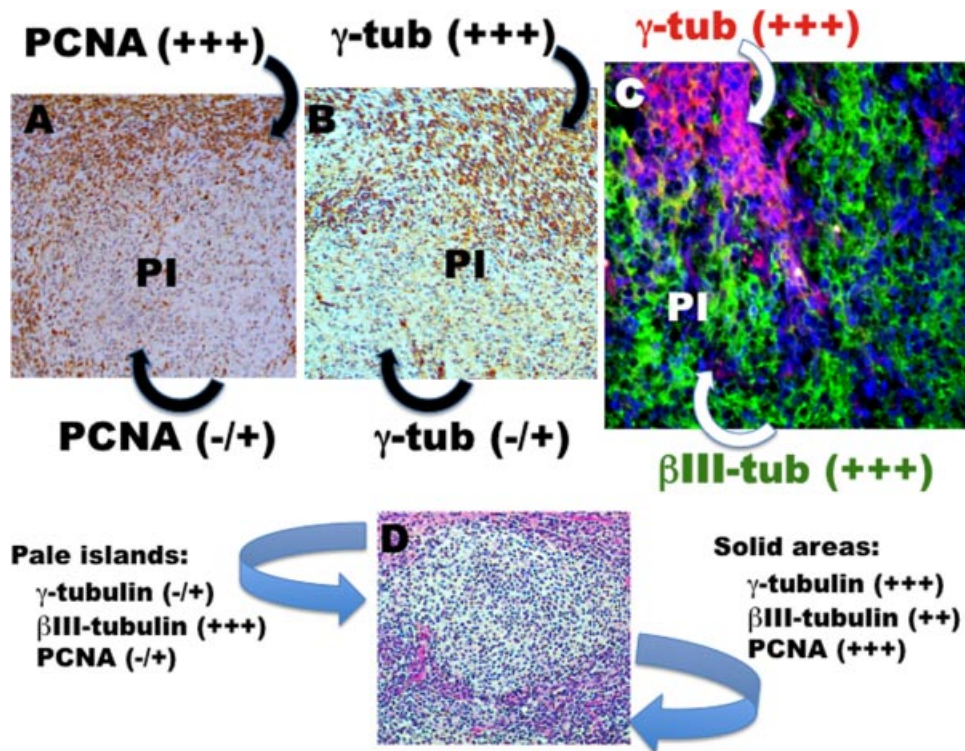


**Fig. 4.** Differential patterns of immunolocalization of proliferating cell nuclear antigen (PCNA), γ-tubulin, and βIII-tubulin in nodular/desmoplastic medulloblastomas. Co-distribution of PCNA and γ-tubulin is prominent in sheets of poorly differentiated cells, when compared with the pale islands (PI) which are, for the most part, PCNA- and γ-tubulin-negative (A,B). Part C depicts the inverse pattern of localization of γ-tubulin and βIII-tubulin by immunofluorescence microscopy. Part D is a schematic depiction of the differential patterns of distribution of γ-tubulin, βIII-tubulin, and PCNA in relation to the histologic components of nodular/desmoplastic medulloblastomas. Immunoreactivity is rated as follows: –, no staining; +, labeling of a small number of tumor cells (LI <20%); ++, labeling of an intermediate number of tumor cells (LI: 20–60%); +++, labeling of a large number of tumor cells (LI ≥60%). ABC peroxidase with hematoxylin counterstain (A,B), immunofluorescence (C), hematoxylin and eosin (D). Original magnifications: A–D 200×.

neuroblastic tumors of the central and peripheral nervous systems (Katsetos et al., 1989, 1995b, 2003a,b,c). Although γ-tubulin is co-expressed with βIII-tubulin in subpopulations of poorly differentiated medulloblastoma cells, these two proteins exhibit distinct patterns of compartmentalization and subcellular sorting in relation to neuronal differentiation.

**Expression of γ-tubulin in medulloblastomas is inversely related to neuritogenesis**

A morphologic comparison of immunoreactivity profiles of γ-tubulin with βIII-tubulin in clinical tumor samples has revealed that both γ-tubulin and βIII-tubulin are widely expressed in medulloblastomas but in distinct patterns of cellular distribution. Immunoreactivity for γ-tubulin was pervasive among poorly differentiated PCNA-positive proliferating tumor cells and was significantly decreased, or absent, in islands of differentiating tumor cells characterized by elaboration of elongated axon-like processes and a very low PCNA LI. This pattern of γ-tubulin expression, which is inversely related to morphologic differentiation (neuritogenesis), recapitulates the lack of this protein in developing axons and dendrites of cultured rat sympathetic neurons (Baas and Joshi, 1992). On the other hand, γ-tubulin was detected in neurite-like processes of murine P19 embryonal carcinoma cells induced by all-trans retinoic acid to undergo neuronal differentiation (Macurek et al., 2008). Further studies are needed to determine whether the microtubules in neurite-like processes of differentiating

medulloblastoma cells (Katsetos et al., 1988) originate at the centrosomes or are nucleated in situ in the growing cell processes.

**Medulloblastoma cell lines differ in expression and distribution of γ-tubulin and βIII-tubulin**

Non-neoplastic interphase cells contain one or two juxtannuclear centrosomes typified by pericentriolar staining for γ-tubulin, and usually a relatively small amount of cytosolic soluble fraction (Nováková et al., 1996; Katsetos et al., 2006). Although this typical pattern of γ-tubulin distribution was found in DAOY cells, highly prominent diffuse cytoplasmic γ-tubulin staining was detected in D283 Med cells. This pattern of γ-tubulin overexpression mirrors what has been previously described in other cell lines derived from malignant brain tumors such as glioblastomas multiforme (Katsetos et al., 2006, 2007, 2009a) indicating that, under neoplastic conditions, γ-tubulin is either incorporated into insoluble (oligomeric) aggregates, associated with membranous components, or is part of an increased cytoplasmic pool. βIII-Tubulin exhibited a partial cytoskeletal distribution associated with cytoplasmic microtubule arrays (DAOY cells) as well as a diffuse cytosolic localization without incorporation into microtubule polymers (DAOY cells and D283 Med cells). Similar immunofluorescence staining patterns for γ-tubulin and βIII-tubulin were found in both cell lines under different fixation conditions. Overall, immunofluorescence experiments revealed a higher level of

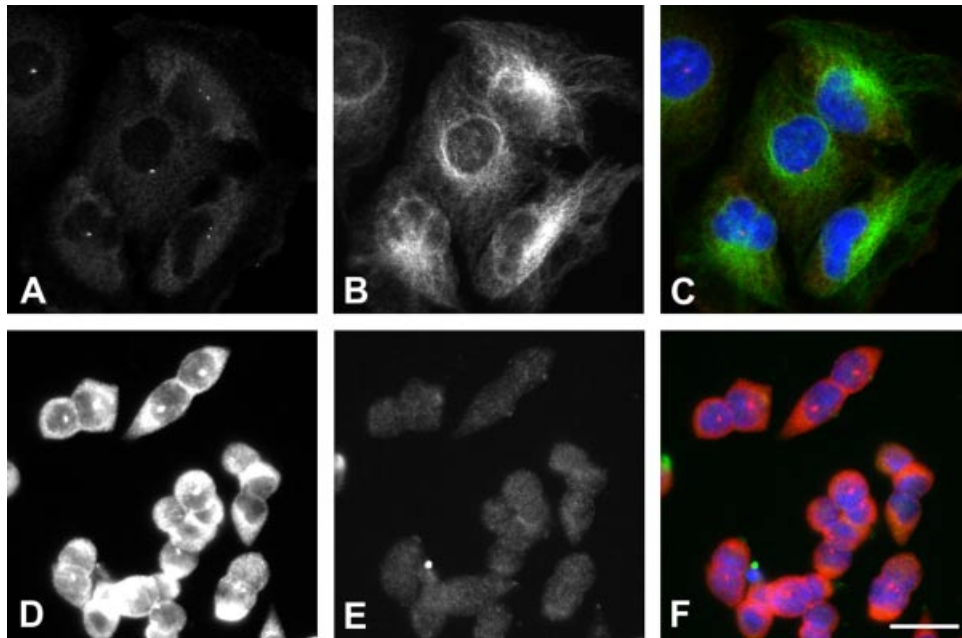


**Fig. 5.** Localization of  $\gamma$ -tubulin and  $\beta$ III-tubulin in interphase DAOY (A–C) and D283 Med (D–F) cells.  $\gamma$ -Tubulin (red; A,D) and  $\beta$ III-tubulin (green; B,E) staining is combined in merged images (C,F). DAPI (blue). Methanol fixation. Images were captured under identical conditions and processed in the same manner. Scale bar: 20  $\mu$ m.

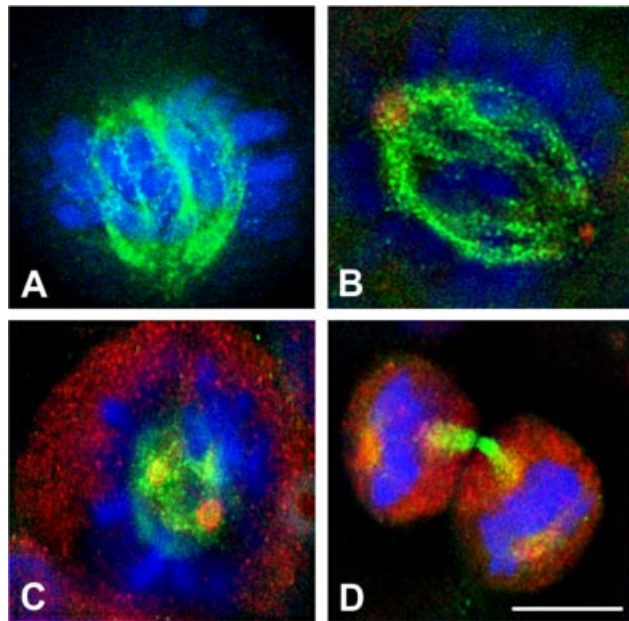


**Fig. 6.** Localization of  $\beta$ III-tubulin and  $\gamma$ -tubulin in mitotic DAOY cells. Cells in metaphase (A,B), anaphase (C), and telophase/cytokinesis (D) were stained for  $\beta$ III-tubulin (green; A–D) and  $\gamma$ -tubulin (red; B–D). DAPI (blue). Note  $\beta$ III-tubulin immunolabeled mitotic spindle microtubules of cells in metaphase and anaphase flanked by two  $\gamma$ -tubulin immunoreactive centrosomes (B,C) as well as in the midbody of cytokinesis (D). Formaldehyde fixation followed by Triton X-100 extraction. Scale bar: 10  $\mu$ m.

$\gamma$ -tubulin and a lower level of  $\beta$ III-tubulin staining in D283 Med cells when compared with DAOY cells. These findings were corroborated by immunoblotting experiments and RT-qPCR. Collectively, these data might reflect higher proliferative and metastasizing potential of D283 Med cells, which express high levels of c-Myc mRNA and protein without genomic amplification (Siu et al., 2003). Overexpression of c-Myc is associated with tumor anaplasia and worse clinical outcomes in patients with medulloblastomas (Eberhart et al., 2004). Cho et al. (2010) have recently shown that aggressive breast cancer cell lines with metastatic potential exhibit a diffuse and soluble, as well as distinctly more dispersive, subcellular localization of  $\gamma$ -tubulin when compared with non-invasive cell lines in which the localization of this protein is largely centrosomal.

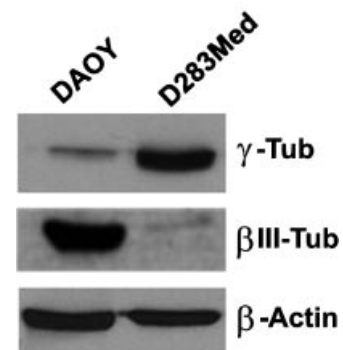


**Fig. 7.** Expression of  $\gamma$ -tubulin and  $\beta$ III-tubulin in asynchronously growing DAOY and D283 Med medulloblastoma cells.  $\beta$ -Actin served as loading control.



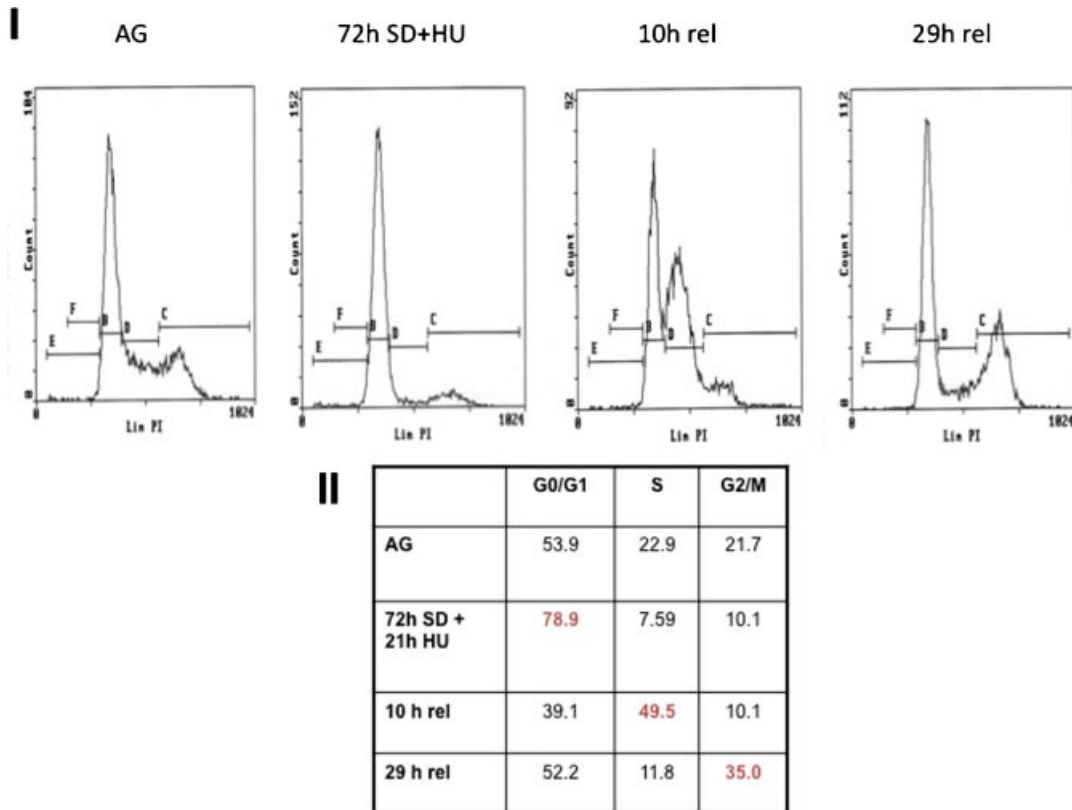


**Fig. 8.** Cell cycle profiles of DAOY cells. Part I depicts asynchronous growth (AG), after 72 h serum deprivation and hydroxyurea treatment (72 h SD + HU; synchronized G0/G1 cells), after 10 h release from the G0/G1 phase (10 h rel; synchronized S-phase cells) and after 29 h release from the G0/G1 phase (29 h rel; G2/M synchronous cells). Cells were replated and refed with serum to restart their cellular cycle (X—relative DNA content, Y—number of cells). Part II shows the distribution (%) of the cells in the different phases of the cell cycle for each condition.

**Differential localization of  $\gamma$ -tubulin and  $\beta$ III-tubulin in mitotic cells**

Previous studies have shown that, in mitotic cells,  $\gamma$ -tubulin is distributed along spindle fibers (Lajoie-Mazenc et al., 1994; Nováková et al., 1996) and during cytokinesis in the midbodies (Julian et al., 1993; Nováková et al., 1996). In mitotic DAOY and D283 Med cells,  $\gamma$ -tubulin was not only localized in spindle poles but also exhibited prominent diffuse cytoplasmic staining. However, the latter may not necessarily reflect a true increase

in the amount of cytoplasmic  $\gamma$ -tubulin, as it may be spuriously accentuated due to the rounded shape of cells in mitosis. Such conclusion was supported by immunoblotting experiment on synchronized DAOY cells, where no changes in the amounts of  $\gamma$ -tubulin were detected in different stages of cell cycle.

Localization of  $\beta$ III-tubulin in mitotic spindle microtubules, which is, to our knowledge, reported for the first time in the context of medulloblastomas, has been previously reported in neuroblasts (neuronal precursors) of rat sensory and sympathetic ganglia (Memberg and Hall, 1995) and in cancerous epithelial, mesenchymal, and nerve sheath cells (Jouhilahti et al., 2008). Further studies are required to determine the extent to which  $\beta$ III-tubulin is expressed in the mitotic spindles as a universal phenomenon of neoplasia or whether it exhibits tumor-type selectivity. Also, it remains to be elucidated whether the expression of this protein in spindle microtubules of neuronal versus non-neuronal tumors bears any biological or clinical significance. The detection of  $\beta$ III-tubulin in mitotic spindles of medulloblastoma cells has potential implications in cancer chemotherapy, as microtubules enriched in  $\beta$ III-tubulin are known to exhibit increased dynamic instability, and chemoresistance to tubulin-binding agents, especially taxanes (reviewed in Katsetos et al., 2009b).

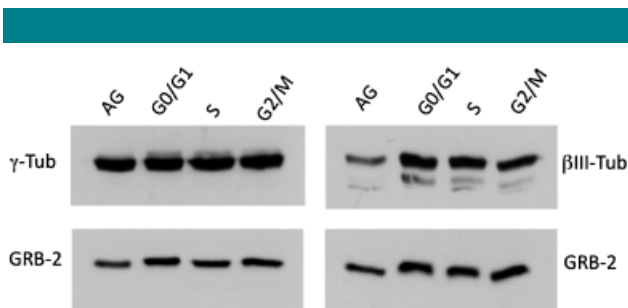


**Fig. 9.** Protein extracts from DAOY cells, corresponding to each cell cycle profile, were analyzed by immunoblots. The results show a comparable level of expression of both  $\gamma$ - and  $\beta$ III-tubulins in G0/G1, S, and G2/M phases of cell cycle.

**Expression of the two  $\gamma$ -tubulin functional genes in medulloblastomas**

When compared with the multiple genes encoding for  $\beta$ -tubulin isotypes (Ludueña and Banerjee, 2008), there are only two

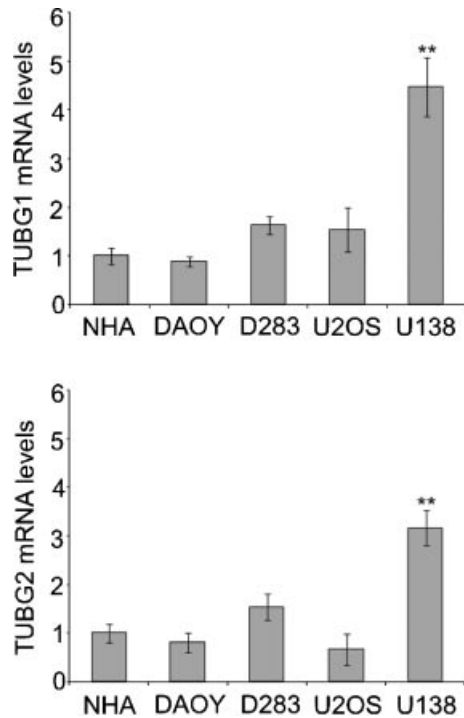


**Fig. 10.** Transcription of genes for  $\gamma$ -tubulin 1 (TUBG1) and  $\gamma$ -tubulin 2 (TUBG2) in medulloblastoma cell lines DAOY and D283 Med (D283), osteosarcoma cell line U-2OS, and glioblastoma cell line U138MG (U138) relative to the level in normal human astrocytes (NHA) (explanted mid-gestational human fetal astrocytes with stem cell properties). Data are presented as the mean fold change  $\pm$  SEM obtained from two independent experiments with triplicate samples. Mean values different from NHA levels are indicated: \*\* $P < 0.01$ .

functional genes in mammalian cells (TUBG1, TUBG2) that code very similar  $\gamma$ -tubulin species (Wise et al., 2000; Yuba-Kubo et al., 2005). TUBG1 is ubiquitously expressed in all cell types, whereas TUBG2 is expressed mainly in the brain (Yuba-Kubo et al., 2005). However, in the present study, both  $\gamma$ -tubulin genes were expressed at comparable levels in medulloblastoma cell lines. RT-qPCR experiments have revealed that the expression of mRNAs for TUBG1 and TUBG2 in medulloblastoma cell lines is decreased when compared with the TUBG1 and TUBG2 transcript levels of the human glioblastoma cell line U138MG. Similarly in the other tested glioblastoma cell lines, namely, T98G and U138MG, the expression of mRNAs for TUBG1 and TUBG2 was higher than in medulloblastoma cell lines (V. Sládková, unpublished data). Tumor cells can, therefore, substantially differ in the expression of  $\gamma$ -tubulins.

Molecular profiling has revealed changes in the expression of both TUBG1 and TUBG2 genes in breast cancer cells (Orsetti et al., 2004), prostate cancer cells (Li et al., 2005), thyroid carcinoma (Montero-Conde et al., 2008), gliomas (Rickman et al., 2001), and pediatric pilocytic astrocytomas (Potter et al., 2008). A recent clinicopathologic study has shown that  $\gamma$ -tubulin may be a promising marker of recurrence of squamous cell carcinoma of the larynx (Syed et al., 2009). Increased  $\gamma$ -tubulin expression occurs in preinvasive mammary cancer lesions and infiltrating carcinomas of the breast (Liu et al., 2009; Niu et al., 2009).

Collectively taken, our findings indicate that in the context of medulloblastoma, overexpression of  $\gamma$ -tubulin is associated with poorly differentiated, actively proliferating tumor cells

and is inversely associated with tumor neurogenesis. The lack or paucity of  $\gamma$ -tubulin distribution in areas of tumor neurogenesis of nodular/desmoplastic medulloblastomas recapitulates normal axogenesis. Overexpression of  $\gamma$ -tubulin in the context of medulloblastomas may be a molecular signature of phenotypic dedifferentiation (anaplasia) and may be linked to tumor progression and worse clinical outcomes. Further studies are indicated in a large patient cohort to investigate the potential of  $\gamma$ -tubulin as a promising tumor marker.

#### Acknowledgments

This work was supported in part by the Sbarro Health Research Organization (S.H.R.O.) ([www.shro.org](http://www.shro.org)) and Human Health Foundation ([www.hhfonlus.org](http://www.hhfonlus.org)) (to A.G.), by Grant IM683780500 from Ministry of Education, Youth and Sports of the Czech Republic, Grant 204/09/1777 from Grant Agency of the Czech Republic, Grant KAN200520701 from GA AVCR and by Institutional Research Support (AVOZ 50520514) (to P.D., E.D., and V.M.), and by a grant from the St. Christopher's Foundation for Children (to C.D.K.).

#### Literature Cited

- Alexander JE, Hunt DF, Lee MK, Shabanowitz J, Michel H, Berlin SC, MacDonald TL, Sundberg RJ, Rebhun LI, Frankfurter A. 1991. Characterization of posttranslational modifications in neuron-specific class III  $\beta$ -tubulin by mass spectrometry. *Proc Natl Acad Sci USA* 88:4685–4689.
- Baas PW, Joshi HC. 1992.  $\gamma$ -Tubulin distribution in the neuron: Implications for the origins of neuritic microtubules. *J Cell Biol* 119:171–178.
- Binarová P, Cenková V, Hause B, Kubátová E, Lysák M, Doležel J, Bögre L, Dráber P. 2000. Nuclear  $\gamma$ -tubulin during acentriolar plant mitosis plant cell. *12:433–442*.
- Bouissou A, Vérolet C, Sousa A, Sampaio P, Wright M, Sunkel CE, Merdes A, Raynaud-Messina B. 2009.  $\gamma$ -Tubulin ring complexes regulate microtubule plus end dynamics. *J Cell Biol* 187:327–334.
- Bugnard E, Zaal KJ, Ralston E. 2005. Reorganization of microtubule nucleation during muscle differentiation. *Cell Motil Cytoskeleton* 60:1–13.
- Chabin-Brion K, Marceiller J, Perez F, Settegrana C, Drechou A, Durand G, Pous C. 2001. The Golgi complex is a microtubule-organizing organelle. *Mol Biol Cell* 12:2047–2060.
- Cho EH, Whipple RA, Matrone MA, Balzer EM, Martin SS. 2010. Delocalization of  $\gamma$ -tubulin due to increased solubility in human breast cancer cell lines. *Cancer Biol Ther* (in press).
- Dráber P, Dráberová E, Linhartová I, Viklický V. 1989. Differences in the exposure of C and N-terminal tubulin domains in cytoplasmic microtubules detected with domain-specific monoclonal antibodies. *J Cell Sci* 92:519–528.
- Dráber P, Dráberová E, Nováková M. 1995. Stability of monoclonal IgM antibodies freeze-dried in the presence of trehalose. *J Immunol Methods* 181:37–43.
- Dráberová E, Del Valle L, Gordon J, Marková V, Šmejkalová B, Bertrand L, de Chadarevian JP, Agamanolis DP, Legido A, Khalili K, Dráber P, Katsetos CD. 2008. Class III  $\beta$ -tubulin is constitutively coexpressed with glial fibrillary acidic protein and nestin in midgestational human fetal astrocytes: Implications for phenotypic identity. *J Neuropathol Exp Neurol* 67:341–354.
- Dryková D, Cenková V, Sulimenko V, Volc J, Dráber P, Binarová P. 2003. Plant  $\gamma$ -tubulin interacts with  $\alpha$ beta-tubulin dimers and forms membrane-associated complexes. *Plant Cell* 15:465–480.
- Eberhart CG, Kaufman WE, Tihan T, Burger PC. 2001. Apoptosis, neuronal maturation, and neurotrophin expression within medulloblastoma nodules. *J Neuropathol Exp Neurol* 60:462–469.
- Eberhart CG, Kepner JL, Goldthwaite PT, Kun LE, Duffner PK, Friedman HS, Strother DR, Burger PC. 2002. Histopathologic grading of medulloblastomas: A Pediatric Oncology Group study. *Cancer* 94:552–560.
- Eberhart CG, Kratz J, Wang Y, Summers K, Stearns D, Cohen K, Dang CV, Burger PC. 2004. Histopathological and molecular prognostic markers in medulloblastoma: c-myc, N-myc, TrkC, and anaplasia. *J Neuropathol Exp Neurol* 63:441–449.
- Efimov A, Kharitonov A, Efimova N, Loncarek J, Miller PM, Andreyeva N, Gleeson P, Galjart N, Maia AR, McLeod IX, Yates JR III, Maiato H, Khodjakov A, Akhmanova A, Kaverina I. 2007. Asymmetric CLASP-dependent nucleation of noncentrosomal microtubules at the trans-Golgi network. *Dev Cell* 12:917–930.
- He XM, Skapek SX, Wikstrand CJ, Friedman HS, Trojanowski JQ, Kemshead JT, Coakham BH, Bigner SH, Bigner DD. 1989. Phenotypic analysis of four human medulloblastoma cell lines and transplantable xenografts. *J Neuropathol Exp Neurol* 48:48–68.
- Jouhilahti EM, Peltonen S, Peltonen J. 2008. Class III  $\beta$ -tubulin is a component of the mitotic spindle in multiple cell types. *J Histochem Cytochem* 56:1113–1119.
- Julian M, Tollon Y, Lajoie-Mazenc I, Moisan A, Mazarguil H, Puget A, Wright M. 1993.  $\gamma$ -Tubulin participates in the formation of the midbody during cytokinesis in mammalian cells. *J Cell Sci* 105:145–156.
- Katsetos CD, Burger PC. 1994. Medulloblastoma. *Semin Diagn Pathol* 11:85–97.
- Katsetos CD, Liu HM, Zacks SI. 1988. Immunohistochemical and ultrastructural observations on Homer Wright (neuroblastic) rosettes and the "pale islands" of human cerebellar medulloblastomas. *Hum Pathol* 19:1219–1227.
- Katsetos CD, Herman MM, Frankfurter A, Gass P, Collins VP, Walker CC, Roseberg S, Barnard RO, Rubinstein LJ. 1989. Cerebellar desmoplastic medulloblastomas. A further immunohistochemical characterization of the reticulin-free pale islands. *Arch Pathol Lab Med* 113:1019–1029.
- Katsetos CD, Frankfurter A, Christakos S, Manca LL, Vlachos I, Ulrich H. 1993. Differential localization of class III  $\beta$ -tubulin isotype and calbindin-D28k defines distinct neuronal types in the developing human cerebellar cortex. *J Neuropathol Exp Neurol* 52:655–666.

- Katsetos CD, Herman MM, Krishna L, Vender JR, Vinoses SA, Agamanolis DP, Schiffer D, Burger PC, Ulrich H. 1995a. Calbindin-D28k in subsets of medulloblastomas and in the human medulloblastoma cell line D283 Med. Arch Pathol Lab Med 119:734-743.
- Katsetos CD, Krishna L, Frankfurter A, Karkavelas G, Wolfe DE, Valsamis MP, Schiffer D, Vlachos I, Ulrich H. 1995b. A cytomorphological scheme of differentiating neuronal phenotypes in cerebellar medulloblastomas based on immunolocalization of class III  $\beta$ -tubulin isotype (bIII) and proliferating cell nuclear antigen (PCNA)/cyclin. Clin Neuropathol 14:72-81.
- Katsetos CD, Karkavelas G, Herman MM, Vinoses SA, Provencio J, Spano AJ, Frankfurter A. 1998. Class III  $\beta$ -tubulin isotype (bIII) in the adrenal medulla: I. Localization in the developing human adrenal medulla. Anat Rec 250:335-343.
- Katsetos CD, Kontogeorgos G, Geddes JF, Herman MM, Tsimara-Papastamatiou H, Yu Y, Sakkas LI, Tsokos M, Patchefsky AS, Ehya H, Cooper HS, Provencio J, Spano AJ, Frankfurter A. 2000. Differential distribution of the neuron-associated class III  $\beta$ -tubulin in neuroendocrine lung tumors. Arch Pathol Lab Med 124:535-544.
- Katsetos CD, Del Valle L, Legido A, de Chadarevian JP, Perentes E, Mörk SJ. 2003a. On the neuronal/neuroblastic nature of medulloblastomas: A tribute to Pio del Rio Hortega and Moises Polak. Acta Neuropathol 105:1-13.
- Katsetos CD, Herman MM, Mörk SJ. 2003b. Class III  $\beta$ -tubulin in human development and cancer. Cell Motil Cytoskeleton 55:77-96.
- Katsetos CD, Legido A, Perentes E, Mörk SJ. 2003c. Class III  $\beta$ -tubulin isotype: A key cytoskeletal protein at the crossroads of developmental neurobiology and tumor neuropathology. J Child Neurol 18:851-866.
- Katsetos CD, Reddy G, Dráberová E, Šmejkalová B, Del Valle L, Ashraf Q, Tadevosyan A, Yelin K, Maraziotis T, Mishra OP, Mörk S, Legido A, Nissanov J, Baas PW, de Chadarevian JP, Dráber P. 2006. Altered cellular distribution and subcellular sorting of  $\gamma$ -tubulin in diffuse astrocytic gliomas and human glioblastoma cell lines. J Neuropathol Exp Neurol 65:465-477.
- Katsetos CD, Dráberová E, Šmejkalová B, Reddy G, Bertrand L, de Chadarevian JP, Legido A, Nissanov J, Baas PW, Dráber P. 2007. Class III  $\beta$ -tubulin and  $\gamma$ -tubulin are co-expressed and form complexes in human glioblastoma cells. Neurochem Res 32:1387-1398.
- Katsetos CD, Dráberová E, Legido A, Dráber P. 2009a. Tubulin targets in the pathobiology and therapy of glioblastoma multiforme. II.  $\gamma$ -tubulin. J Cell Physiol 221:514-520.
- Katsetos CD, Dráberová E, Legido A, Dumontet C, Dráber P. 2009b. Tubulin targets in the pathobiology and therapy of glioblastoma multiforme. I. class III  $\beta$ -tubulin. J Cell Physiol 221:505-513.
- Laemmli UK. 1970. Cleavage of structural proteins during the assembly of the head of bacteriophage T4. Nature 227:680-685.
- Lajoie-Mazenc I, TOLLON I, Détraves C, Julian M, Moisan A, Gueth-Hallonet C, Debec A, Lajoie-Passador I, Puget A, Mazarguil H, Raynaud-Messina B, Wright M. 1994. Recruitment of antigenic  $\gamma$ -tubulin during mitosis in animal cells: Presence of  $\gamma$ -tubulin in the mitotic spindle. J Cell Sci 107:2825-2837.
- Lee MK, Rebhun LI, Frankfurter A. 1990a. Posttranslational modification of class III  $\beta$ -tubulin. Proc Natl Acad Sci USA 87:7195-7199.
- Lee MK, Tuttle JB, Rebhun LI, Cleveland DW, Frankfurter A. 1990b. The expression and posttranslational modification of a neuron-specific  $\beta$ -tubulin isotype during chick embryogenesis. Cell Motil Cytoskeleton 17:118-132.
- Leguy R, Melki R, Pantaloni D, Carlier MF. 2000. Monomeric  $\gamma$ -tubulin nucleates microtubules. J Biol Chem 275:21975-21980.
- Li PK, Xiao Z, Hu Z, Pandit B, Sun Y, Sackett DL, Werbovets K, Lewis A, Johnson J. 2005. Conformationally restricted analogs of Combretastatin A-4 derived from SU5416. Bioorg Med Chem Lett 15:5382-5385.
- Libusová L, Sulimenko T, Sulimenko V, Hozák P, Dráber P. 2004.  $\gamma$ -Tubulin in Leishmania: Cell cycle-dependent changes in subcellular localization and heterogeneity of its isoforms. Exp Cell Res 295:375-386.
- Liu T, Niu Y, Yu Y, Liu Y, Zhang F. 2009. Increased gamma-tubulin expression and P16INK4A promoter methylation occur together in preinvasive lesions and carcinomas of the breast. Ann Oncol 20:441-448.
- Louis DN, Ohgaki H, Wiestler OD, Cavenee WK, Burger PC, Jouvet A, Scheithauer BW, Kleihues P. 2007. The 2007 WHO classification of tumours of the central nervous system. Acta Neuropathol 114:97-109.
- Ludueña RF, Banerjee A. 2008. The isotypes of tubulin: Distribution and functional significance. In: Fojo T, editor. Cancer drug discovery and development: the role of microtubules in cell biology, neurobiology, and oncology. Totowa, NJ: Humana Press. pp 123-175.
- Macurek L, Dráberová E, Richterová V, Sulimenko V, Sulimenko T, Dráberová L, Marková V, Dráber P. 2008. Regulation of microtubule nucleation from membranes by complexes of membrane-bound gamma-tubulin with Fyn kinase and phosphoinositide 3-kinase. Biochem J 416:421-430.
- Memberg SP, Hall AK. 1995. Dividing neuron precursors express neuron-specific tubulin. J Neurobiol 27:26-43.
- Montero-Conde C, Martín-Campos JM, Lerma E, Gimenez G, Martínez-Guitarte JL, Combalia N, Montaner D, Matias-Guiu X, Dopazo J, de Leiva A, Robledo M, Mauricio D. 2008. Molecular profiling related to poor prognosis in thyroid carcinoma. Combining gene expression data and biological information. Oncogene 27:1554-1561.
- Moritz M, Braunfeld MB, Sedat JW, Alberts B, Agard DA. 1995. Microtubule nucleation by  $\gamma$ -tubulin-containing rings in the centrosome. Nature 378:638-640.
- Moritz M, Zheng Y, Alberts BM, Oegema K. 1998. Recruitment of the  $\gamma$ -tubulin ring complex to *Drosophila* salt-stripped centrosome scaffolds. J Cell Biol 142:775-786.
- Moudjou M, Bordes N, Paintrand M, Bornens M. 1996.  $\gamma$ -Tubulin in mammalian cells: The centrosomal and the cytosolic forms. J Cell Sci 109:875-887.
- Müller H, Fogeron ML, Lehmann V, Lehrach H, Lange BM. 2006. A centrosome-independent role for  $\gamma$ -TuRC proteins in the spindle assembly checkpoint. Science 314:654-657.
- Niu Y, Liu T, Tse GM, Sun B, Niu R, Li HM, Wang H, Yang Y, Ye X, Wang Y, Yu Q, Zhang F. 2009. Increased expression of centrosomal alpha,  $\gamma$ -tubulin in atypical ductal hyperplasia and carcinoma of the breast. Cancer Sci 100:580-587.
- Nováková M, Dráberová E, Schürmann W, Czihak G, Vildický V, Dráber P. 1996.  $\gamma$ -Tubulin redistribution in taxol-treated mitotic cells probed by monoclonal antibodies. Cell Motil Cytoskeleton 33:38-51.
- Orsetti B, Nugoli M, Cervera N, Lasorsa L, Chuchana P, Ursule L, Nguyen C, Redon R, du Manoir S, Rodriguez C, Theillet C. 2004. Genomic and expression profiling of chromosome 17 in breast cancer reveals complex patterns of alterations and novel candidate genes. Cancer Res 64:6453-6460.
- Paluh JL, Nogales E, Oakley BR, McDonald K, Pidoux AL, Cande WZ. 2000. A mutation in  $\gamma$ -tubulin alters microtubule dynamics and organization and is synthetically lethal with the kinesin-like protein pklp. Mol Biol Cell 11:1225-1239.
- Peyrl A, Krapfenbauer K, Slavc I, Yang JW, Strobel T, Lubec G. 2003. Protein profiles of medulloblastoma cell lines DAOY and D283: Identification of tumor-related proteins and principles. Proteomics 3:1781-1800.
- Potter N, Karakoula A, Phipps KP, Harkness W, Hayward R, Thompson DN, Jacques TS, Harding B, Thomas DG, Palmer RV, Rees J, Darling J, Warr TJ. 2008. Genomic deletions correlate with underexpression of novel candidate genes at six loci in pediatric pilocytic astrocytoma. Neoplasia 10:757-772.
- Prigozhina NL, Walker RA, Oakley CE, Oakley BR. 2001.  $\gamma$ -Tubulin and the C-terminal motor domain kinesin-like protein, KLP4, function in the establishment of spindle bipolarity in *Aspergillus nidulans*. Mol Biol Cell 12:3161-3174.
- Raynaud-Messina B, Merdes A. 2007.  $\gamma$ -tubulin complexes and microtubule organization. Curr Opin Cell Biol 19:24-30.
- Read TA, Hegedus B, Wechsler-Reya R, Gutmann DH. 2006. The neurobiology of neurooncology. Ann Neurol 60:3-11.
- Rickman DS, Bobek MP, Misk DE, Kuick R, Blaivas M, Kurnit DM, Taylor J, Hanash SM. 2001. Distinctive molecular profiles of high-grade and low-grade gliomas based on oligonucleotide microarray analysis. Cancer Res 61:6885-6891.
- Rodriguez AS, Batac J, Killilea AN, Filopei J, Simeonov DR, Lin I, Paluh JL. 2008. Protein complexes at the microtubule organizing center regulate bipolar spindle assembly. Cell Cycle 7:1246-1253.
- Schnackenberg BJ, Palazzo RE. 2001. Reconstitution of centrosome microtubule nucleation in *Spizula*. Methods Cell Biol 67:149-165.
- Schröder J, Kautz K, Wernicke W. 2002.  $\gamma$ -Tubulin in barley and tobacco: Sequence relationship and RNA expression patterns in developing leaves during mitosis and post-mitotic growth. Plant Cell Physiol 43:224-229.
- Siu IM, Lal A, Blankenship JR, Aldosari N, Riggins GJ. 2003. c-Myc promoter activation in medulloblastoma. Cancer Res 63:4773-4776.
- Sulimenko V, Sulimenko T, Poznanovic S, Nechiporuk-Zloy V, Böhm K, Macúrek L, Unger E, Dráber P. 2002. Association of brain  $\gamma$ -tubulins with  $\alpha$  $\beta$ -tubulin dimers. Biochem J 365:889-895.
- Syed MI, Syed S, Minty F, Harrower S, Singh J, Chin A, McLellan DR, Parkinson EK, Clark LJ. 2009. Gamma tubulin: A promising indicator of recurrence in squamous cell carcinoma of the larynx. Otolaryngol Head Neck Surg 140:498-504.
- Towbin H, Staehelin T, Gordon J. 1979. Electrophoretic transfer of proteins from polyacrylamide gels to nitrocellulose sheets: Procedure and some applications. Proc Natl Acad Sci USA 76:4350-4354.
- Vardy L, Fujita A, Toda T. 2002. The  $\gamma$ -tubulin complex protein Alp4 provides a link between the metaphase checkpoint and cytokinesis in fission yeast. Genes Cells 7:365-373.
- Wiese C, Zheng Y. 2000. A new function for the  $\gamma$ -tubulin ring complex as a microtubule minus-end cap. Nat Cell Biol 2:358-364.
- Wise DO, Krahe R, Oakley BR. 2000. The  $\gamma$ -tubulin gene family in humans. Genomics 67:164-170.
- Yuba-Kubo A, Kubo A, Hata M, Tsukita S. 2005. Gene knockout analysis of two  $\gamma$ -tubulin isoforms in mice. Dev Biol 282:361-373.
- Zheng Y, Wong ML, Alberts B, Mitchison T. 1995. Nucleation of microtubule assembly by a  $\gamma$ -tubulin-containing ring complex. Nature 378:578-583.
- Zhou J, Shu HB, Joshi HC. 2002. Regulation of tubulin synthesis and cell cycle progression in mammalian cells by  $\gamma$ -tubulin-mediated microtubule nucleation. J Cell Biochem 84:472-483.